ELSEVIER

Chemical Engineering Journal 72 (1999) 153–161

Chemical Engineering Journal

Modelling and analysis of axial flow through and compression of a non-rigid chromatographic bed

Karin C.E. Östergren*, Christian Trägårdh

Department of Food Engineering, Lund University, P.O. Box 124, SE-221 00, Lund, Sweden

Received 2 April 1998; received in revised form 30 October 1998; accepted 4 November 1998

Abstract

Compression and axial flow through a chromatographic column packed with a non-rigid gel have been characterized experimentally and theoretically. A two-dimensional model based on the assumption of elastic deformation of the solid phase and steady-state Darcy flow was modified to include the mechanical forces exerted by the end pieces of the column. Flow–pressure curves were successfully predicted by the model. Pressure drop and radial distribution of the linear velocity at different flow rates, wall friction coefficients and column radii were investigated by computer simulations. It was shown that significant radial variations in the linear velocity may arise near both the outlet and the inlet of the column.

Keywords: Chromatography; Flow; Compression; Particulate bed; Theoretical model

1. Introduction

The optimal design and operation of a chromatographic process require a proper understanding of the kinetics and mass transfer as well as of the hydrodynamics in the chromatographic bed. The optimal use of chromatography is especially important in preparative chromatography where the economy of the process must be taken into account [1]. The intracolumn velocity profile and the local packing structure will set the limits for the column efficiency. Simulations performed by Yun and Guiochon [2] have shown that an axial velocity variation in a column cross-section with a maximum to minimum ratio as small as 1.10 led to considerable changes in the chromatographic band profiles.

The hydrodynamics in a chromatographic bed containing a non-rigid medium is intimately coupled to the mechanical properties of the packed bed. One-dimensional analyses of compression and flow through a chromatographic column have been presented by Joustrua et al. [3], Davies and Bellhouse [4] and Verhoff and Furjanic [5], among others.

Computer simulations provide a useful tool with which experimental findings and theory to be linked, in order to gain an increased understanding of the flow and deformation of chromatographic matrixes (LC or HPLC).

A general, two-dimensional model based on local isotropy and the assumption of elastic deformation of the chromatographic matrix during steady-state flow has been developed by Östergren and Trägårdh [6,7]. The model was found to successfully predict the degree of compression, pressure drop and flow rate for a highly compressible LC-medium packed in an open column.

In the present study the model has been extended to describe a chromatographic bed fixed by an adaptor, making it possible to take into account also the mechanical stress originating from the end pieces of the column. Predicted pressure profiles and flow rates are compared with experimental data. The variations in the axial linear velocity and pressure drop were investigated by computer simulations assuming different conditions in the chromatographic column. The simulations demonstrate the complex interplay between compaction, wall friction and flow rate.

2. Theory

The liquid flow through a chromatographic bed is generally slow, i.e. the particle Reynolds number ($U\rho d_p/\mu$) is less than 1. Assuming constant viscosity, the flow rate per unit cross-sectional area (U_0) is proportional to the hydrodynamic pressure drop according to Darcy's law, which in its general form is [6]

*Corresponding author. Fax: +46-46-2224622; e-mail: karin.ostergren@livstek.lth.se

1385-8947/99/$ – see front matter
PII: S1385-8947(98)00143-0

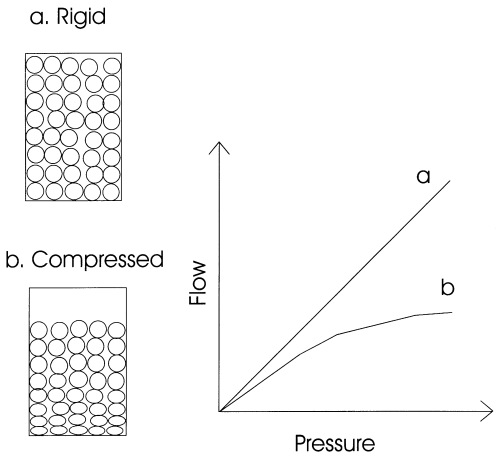

Fig. 1. Flow–pressure characteristics for a column packed with (a) rigid particles and (b) non-rigid particles.

$$\mathbf{U}_0 = -\frac{1}{\mu} k \bigtriangledown P \quad \text{where} \quad \bigtriangledown P = \bigtriangledown p - \rho \mathbf{g} \tag{1}$$

where p is pressure and ρg the gravitational force. The permeability, k, depends on the structure of the interstitial space of the porous medium. In a rigid chromatographic bed, the permeability is independent of position and the pressure drop varies linearly along the column. The situation is different in a non-rigid chromatographic bed. The interstitial void fraction, and thus the permeability, will change along the column due to successive compaction caused by the increase in solid stress. The compaction leads to a non-linear increase in flow rate with pressure drop [1,3,8] according to Fig. 1.

The net force acting on any point in the packed bed is the sum of the forces originating from the flow, the mechanical force caused by end pieces of the column, the friction between the chromatographic bed and the wall and the gravitational force due to density differences between the liquid and the particles. A one-dimensional stress balance across a column segment is shown in Fig. 2. In general, the stress transmitted from the fluid flow is assumed to be equal to the hydrodynamic pressure drop. Due to the wall friction, the solid stress (σ_{xx}) in a column is less than expected from the pressure drop and gravitational force.

The wall friction always opposes the motion at compaction and expansion and the influence of the wall friction decreases with increasing column radius [9]. Shear stresses are not fully transmitted in a particulate medium. Thus, the (shear) stress originating from wall friction is largest at the wall and decreases towards the centre of the column, causing variations in the solid stress (σ_{xx}) also in the in the radial direction [10]. The wall friction is quantified by the wall friction coefficient μ_f [6,11,12].

In chromatographic applications the stress originating from the gravitational force ($\Delta\sigma_g$, Fig. 2) is small compared with the other terms, and can thus be neglected.

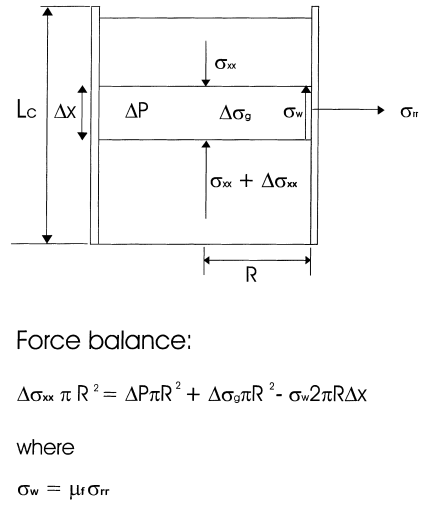

Fig. 2. Forces acting on an axial segment of a column packed with particles and corresponding stress balance. The stresses are positive acting in the positive coordinate direction and the fluid pressure is taken as positive at compression according to the sign convention. L_c = column length, R = column radius, P = Fluid pressure (Eq. (1)), σ_w = particle–wall shear stress, σ_g = stress originating from the gravitational force, $(\rho_{solid} - \rho_{liquid})(1 - \varepsilon)g\Delta x$, σ_{xx} = stress acting in the axial direction and σ_{rr} = stress acting in the radial direction.

2.1. The model

The model describing the flow through and the compaction of a chromatographic bed is based on the theory of Biot [6,7,13] assuming local isotropic conditions and pure elastic deformation of the chromatographic matrix. The model is briefly described below in order to provide the basic concepts. The full, two-dimensional model is described elsewhere [7].

The model is based on the assumption that equilibrium exists between the solid stresses and the fluid pressure according to:

$$\frac{\partial \sigma_{xx}}{\partial x} + \frac{\partial \sigma_{xy}}{\partial y} + \frac{\partial \sigma_{xz}}{\partial z} = \frac{\partial P}{\partial x} \tag{2}$$

where σ_{xy} and σ_{xz} are shear stresses and σ_{xx} is the normal stress acting on a plane according to Fig. 3. P is the fluid pressure as defined in Eq. (1). The sign convention is that the stresses are positive acting in the positive coordinate direction. Thus, unidirectional compression is negative and unidirectional tension is positive. The fluid pressure is taken positive at compression. The deformation can be expressed as strains (ε') or displacements (u). The deformation is related to the stresses according to Hooke's law:

$$\varepsilon'_{xx} = \frac{\partial u_x}{\partial x} = \frac{1}{E}\left[\sigma_{xx} - \nu(\sigma_{yy} + \sigma_{zz})\right]$$

$$\varepsilon'_{yz} = \frac{1}{2}\left(\frac{\partial u_y}{\partial z} + \frac{\partial u_z}{\partial y}\right) = \frac{\sigma_{yz}}{2G} \tag{3}$$

where E is Young's modulus, ν the Poisson ratio and G the

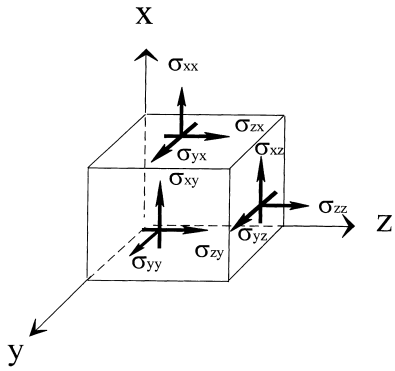

Fig. 3. Stresses acting on an elementary cube in a cartesian coordinate system. σ_{xx}, σ_{yy} and σ_{zz} are normal stresses and σ_{xz} $(=\sigma_{zx})$, σ_{yz} $(=\sigma_{zy})$ and σ_{xy} $(=\sigma_{yx})$ are shear stresses.

shear modulus. The material constants are related to each other according to:

$$G = \frac{E}{2(1+\nu)} \tag{4}$$

i.e. only two constants are required. The material constants are dependent on the degree of compaction [6,14]. The complete, three-dimensional model is obtained by cyclic permutation of the directions given for the stresses, strains and displacements in Eqs. (2) and (3).

Assuming an incompressible mobile phase and steady-state flow the pressure field is given by [13–15]

$$\frac{\partial}{\partial x}\left(\frac{k\rho}{\mu}\frac{\partial P}{\partial x}\right) + \frac{\partial}{\partial y}\left(\frac{k\rho}{\mu}\frac{\partial P}{\partial y}\right) + \frac{\partial}{\partial z}\left(\frac{k\rho}{\mu}\frac{\partial P}{\partial z}\right) = 0 \tag{5}$$

The flow rate per unit area (U_0) is obtained from Eq. (1) and the linear velocity (U) from

$$U = \frac{U_0}{\varepsilon} \tag{6}$$

where ε is the interstitial void fraction

The Kozeny–Carman model was used to describe the permeability (k) using a surface-based, mean particle diameter [6,16,17]

$$k = \frac{d_p^2}{180}\frac{\varepsilon^3}{(1-\varepsilon)^2} \tag{7}$$

The flow in a chromatographic column is axi-symmetric and can be conveniently described using a system of axi-symmetric cylindrical coordinates according to Fig. 4. Eqs. (2)–(7) were thus transformed to a two-dimensional system of axi-symmetric cylindrical coordinates and were then solved numerically using a control–volume method [7].

The boundary conditions imposed on the solid phase and on the fluid phase are summarized in Table 1. For the solid phase a uniform displacement was assumed at the top, since the chromatographic bed is fixed between two planar end pieces. It should be noted that this boundary condition allows for a stress distribution at the inlet cross-section. At the outlet the displacement in the axial direction was

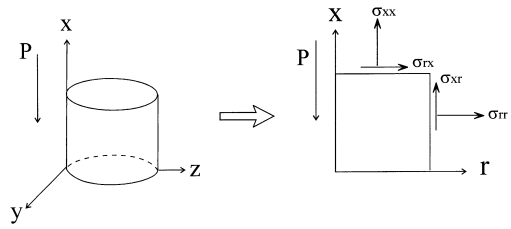

Fig. 4. Stresses acting on an elementary unit after coordinate transformation to axi-symmetric cylindrical coordinates. σ_{rr}, σ_{xx} are normal stresses and σ_{rx} $(=\sigma_{xr})$ are shear stresses.

Table 1
Boundary conditions used in the computer simulations

Boundary	Fluid phase equation	Solid phase equations
Inlet	$x = L_c$	$x = L_c$
	$P(r, L_c) = \Delta P$	$u_x(r, L_c) = \Delta L = L_{co} - L_c$
		$\partial u_r(r, L_c)/\partial x = 0$
Outlet	$x = 0$	$x = 0$
	$P(r, 0) = 0$	$u_x(r, 0) = 0$
		$\partial u_r(r, 0)/\partial x = 0$
Centre	$r = 0$	$r = 0$
	$\partial P(0, x)/\partial r = 0$	$u_r(0, x) = 0$
		$\partial u_r(0, x)/\partial r = 0$, $\partial u_x(0, x)/\partial r = 0$
Wall	$r = R$	$r = R$
	$\partial P(R, x)/\partial r = 0$	$u_r(R, x) = 0$
		$\sigma_{xr}(R, x) = \mu_f \sigma_{rr}(R, x)$

L_{co} – Column length of a non-compressed column.

defined as being zero. The sample radius is constant, and thus the displacement, u_r, was set equal to zero both at the centre and at the column wall. The assumptions of axial symmetry and wall friction give the additional boundary conditions in Table 1. In the flow calculations, the inlet- and outlet pressures, as defined by Eq. (1), were given. It was further assumed that the gel particles did not change in volume [6]. The mechanical properties of the Sephadex gel used in this work are summarized in Table 2. The compression due to the piston stress and the fluid stress was calculated assuming an initially completely relaxed, isotropic column having the same local void fraction everywhere ($\varepsilon = 0.348$).

3. Materials and methods

Sephadex G-75 (Amersham Pharmacia Biotech AB, Sweden) was chosen as the stationary phase since it is highly compressible and will thus serve as a good test for

Table 2
Mechanical properties of Sephadex G-75

E (Pa)	ν (−)	μ_f (−)
$E = 5.63 \times 10^4\varepsilon^2 - 8.39 \times 10^4\varepsilon + 2.77 \times 10^4$	0.27	0.16

E is the Young's modulus, ν is the Poisson ratio, μ_f is the wall friction coefficient and ε is the intergranular void fraction [8].

the model. Further benefits of this chromatographic medium are that its particle volume is not sensitive to the ionic strength of the liquid phase [18] or to mechanical load. The particles have been found not to become deformed permanently after mechanical loading [19] and the particle density has been determined to be approximately 1040 kg/m^3 [20].

The mean wet particle diameter was measured by photomicrography. The number mean diameter was found to be 144 μm and the surface-based mean diameter 178 μm. The void volume was determined by measuring the ratio of superficial to interstitial velocity using dextran sulphate, MW = 500 000, (0.14×10^{-3} kg/l) as tracer. The experiments were performed at constant temperature using deaerated water containing 3×10^{-4} mol/l NaCl.

All experiments were performed in a commercial chromatographic column with a diameter of 0.113 m (BP113, Amersham Pharmacia Biotech AB, Sweden) using the experimental set-up shown in Fig. 5. The column lengths were 0.145, 0.153 and 0.313 m. Six holes ($d = 1$ mm) were made in the column wall at different positions to make the measurement of the axial pressure profile possible. A Mariotte bottle was used to ensure pulse-free flow. The pressure head was set by the elevation of the Mariotte bottle and the mass flow rate was continuously monitored using a balance connected to a computer. The temperature was measured at the outlet of the column using a thermocouple. The distributors consisted of a support plate on which a coarse net, covered with a fine-meshed polyester net was mounted. The mobile phase was fed through the centre of the support plate and the coarse net served as a spacer, ensuring an even distribution of the liquid. The column was packed by pouring a slurry consisting of three volumes of sedimented packing material and one volume of supernatant into the column. The particles were then allowed to pack under a constant flow rate until the desired packing pressure was reached. When the gel particles had settled the adaptor was lowered to the level of the gel bed and was then fixed at that position. After the column was packed the flow direction was reversed. During the experiments, the pressure head was increased step-wise and the flow rate was recorded continuously. All measurements were made at a constant flow rate, i.e. at steady state. At each pressure level the hydrodynamic pressure drop, the flow rate and the outlet temperature were measured. The pressure drop was corrected for the extra-column pressure drop caused by the tubing and the end pieces of the column. All flow rates were re-calculated to correspond to the flow rate of pure water at 20.0°C.

4. Results and discussion

4.1. Experiments

The experiments on the chromatographic column were performed in order to investigate the stability of the gel and to provide experimental data to verify the proposed model. In a previous study [6] the chromatographic packing was characterized in an open column, taking into account the effects of the fluid stress and the wall friction. In the present study also the influence of mechanical stress applied by the column end pieces was investigated.

4.1.1. Stability

In Fig. 6 the results of a typical experimental run are shown. It took between 5 and 10 min to reach a constant flow rate after a change in the applied pressure head.

The initial flow–pressure cycle was characterized by a large irreversible deformation. Elastic deformation, i.e. reproducible flow–pressure curves, was obtained from the third cycle for the column with the highest interstitial void fraction ($\varepsilon_{mean} = 0.283$, Fig. 7(a)) and from the second cycle for the column with the lowest interstitial void fraction ($\varepsilon_{mean} = 0.243$, Fig. 7(b)). Hysteresis behaviour was observed in both cases.

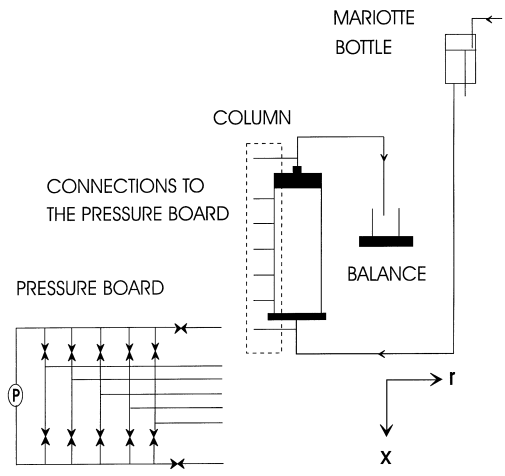

Fig. 5. Experimental set-up.

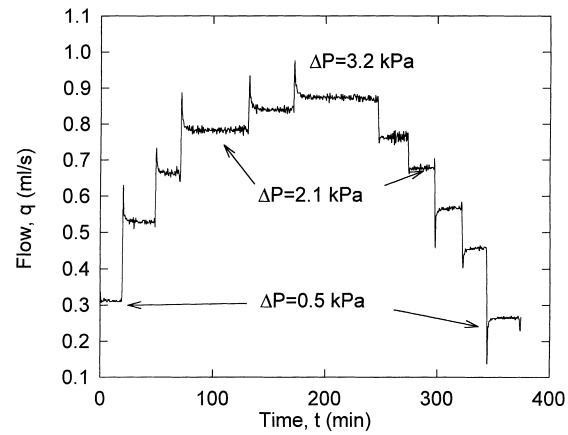

Fig. 6. Typical flow variations as a function of time with increasing and decreasing pressure head. $L_c = 0.313$ m, $\varepsilon_{mean} = 0.237$.

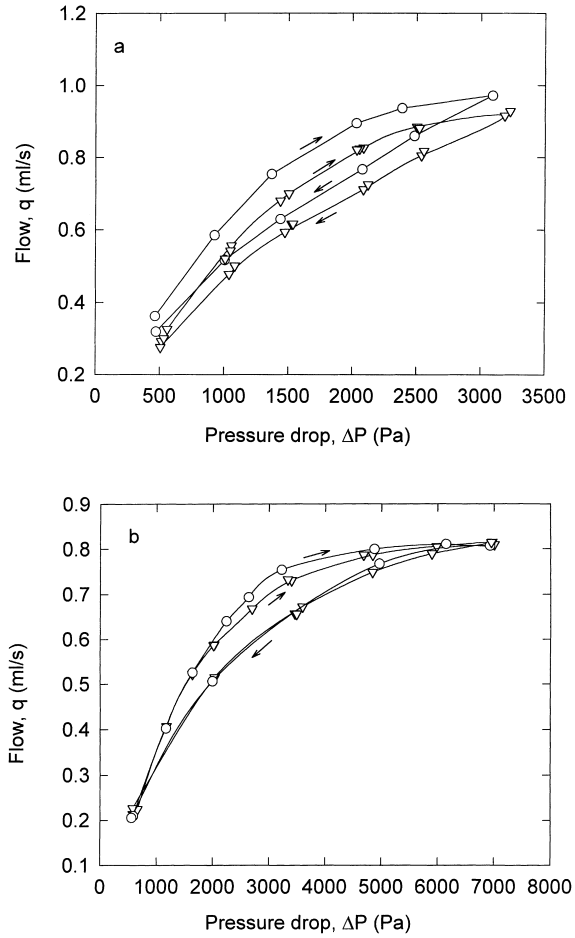

Fig. 7. Initial and stable flow–pressure cycles for two different columns: (a) A column packed at pressure $\Delta P = 3.1$ kPa ($L_c = 0.153$, $\varepsilon_{mean} = 0.283$). (○) Initial cycle, (▽) third–fifth cycles. (b) A column packed at $\Delta P = 8.3$ kPa ($L_c = 0.145$, $\varepsilon_{mean} = 0.243$). (○) Initial cycle, (▽) second–fourth cycles.

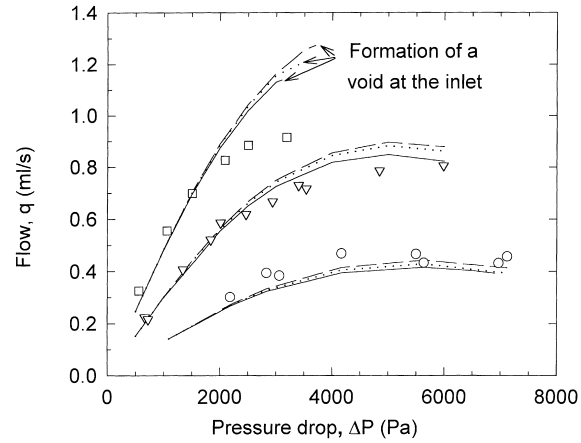

Fig. 8. Measured flow rates (○, ▽, □) and computed flow rates (- -, ···, ———) for a column with $R = 0.0565$ m. The column lengths were 0.15 and 0.31 m and the mean void fractions were 0.24 and 0.28 the flow rates were computed using the material constants in Table 2. Two wall friction coefficients were tested (0.14 and 0.16) as well as the use of an E-module describing the relaxation (Eq. (8)). (○) $L_c = 0.313$ m, $\varepsilon_{mean} = 0.237$ packing pressure: $\Delta P = 8.6$ kPa; (▽) $L_c = 0.145$ m, $\varepsilon_{mean} = 0.243$, packing pressure: $\Delta P = 8.3$ kPa; (□) $L_c = 0.153$ m, $\varepsilon_{mean} = 0.283$. packing pressure: $\Delta P = 3.1$ kPa; (- -) $\mu_f = 0.16$; (···) $\mu_f = 0.14$; (———) $\mu_f = 0.14$, E calculated according to Table 2 and Eq. (8).

4.2. Evaluation of the model

The model was evaluated by comparing experimental and calculated pressure profiles and flow rates.

4.2.1. Flow and pressure calculations

The predicted flow rates for the shorter columns (0.145 and 0.153 m) agreed well with the experimental data at low and moderate pressures, while the predicted flow rates for the 0.313 m column were slightly too low according to Fig. 8. The densely packed columns ($\varepsilon_{mean} = 0.24$) were according to the simulations influenced by a mechanical stress originating from the adaptor even at high flow rates, while the column being less densely packed ($\varepsilon_{mean} = 0.283$) approached open column conditions [6] at high flow rates. In the first case the experimental and predicted flow rates agreed well. For the less densely packed column too high flow rates were predicted, and the difference increased with increasing pressure drop. Close to the packing pressure the predicted flow rate was approximately 30% higher than the experimental value (Fig. 8). This difference is in accordance with the results obtained in the open column study [6] and is believed to be attributed to the permeability model (Eq. (7)), since the flow rate in an open column can be accurately predicted by only changing the constant in Eq. (7) [6].

The Poisson ratio and Young's modulus were verified in a previous study [6]. The sensitivity of the model to changes in the wall friction was investigated by simulations using a wall friction coefficient of 0.14 instead of 0.16. The difference between the simulations was small (Fig. 8).

In a fixed chromatographic bed, both relaxation at the inlet and compression at the outlet occur simultaneously as the pressure head/flow rate is increased. This is in contrast to the conditions for the open column previously studied, where an increased flow rate/pressure head resulted in compression only [6]. The mechanical properties of the gel are slightly different during compression and relaxation [21]. To evaluate the influence of these differences a Young's modulus determined under relaxation [6] was included in the model:

$$E_{relax} = 4.6 \times 10^4 \varepsilon - 6.95 \times 10^4 \varepsilon + 2.35 \times 10^4 \text{ Pa} \qquad (8)$$

The incorporation of a relaxation modulus was found to improve the model only slightly, as can be seen in Fig. 8.

4.2.2. Pressure drop

The computed pressure drop agreed well with values determined experimentally (Fig. 9). The pressure profiles did not change significantly when the wall friction was varied or when the Young's modulus describing the relaxation was added to the model.

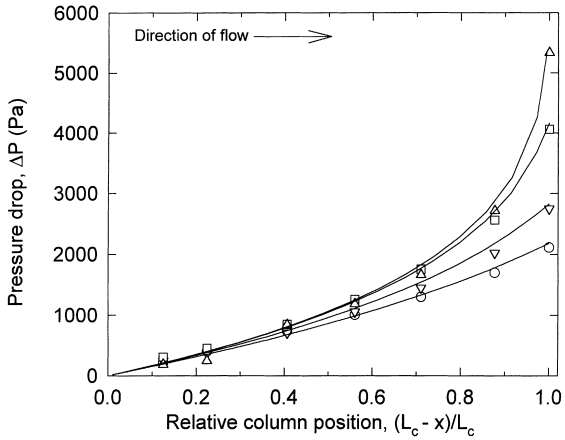

Fig. 9. Measured pressure drop (○, ▽, □, △) and computed values (———) in a chromatographic column ($L_c = 0.313$ m, $R = 0.565$ m; $\varepsilon = 0.237$) packed with Sephadex G-75; (○) $q = 0.26$ ml/s, $\Delta P_{column} = 2.1$ kPa; (▽) $q = 0.34$ ml/s, $\Delta P_{column} = 2.8$ kPa; (□) $q = 0.41$ ml/s, $\Delta P_{column} = 4.1$ kPa, (△) $q = 0.39$ ml/s, $\Delta P_{column} = 5.4$ kPa.

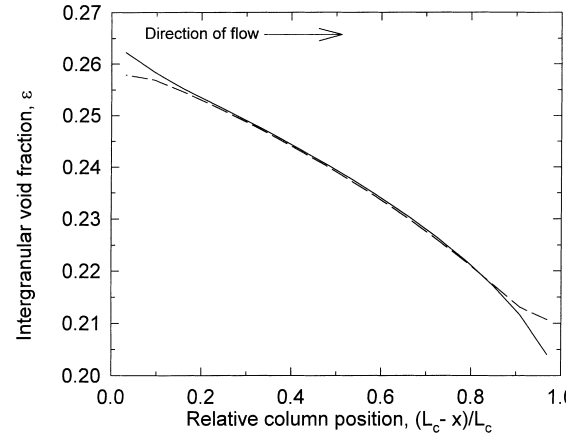

Fig. 10. Computed differences in the intergranular void fraction along the column; (———) centre and (- -) wall. Parameters: $q = 0.26$ ml/s, $R = 0.0565$ m, $L_c = 0.313$ m, $\varepsilon_{mean} = 0.237$, $\mu = 0.001$ Pa s, $\rho = 1000$ kg/m^3. The pressure drop was 2.18 kPa.

4.3. Computer simulations of pressure drop and velocity variations during compression

By computer simulations the influence of the wall friction and the column radius on the pressure drop and linear velocity were investigated for columns under piston stress. The parameters in Table 2 were used in the simulations. The initial conditions were the same as those described previously.

Radial variations in the linear velocity may decrease the separation efficiency. To quantify these variations a wall region being $\Delta r = 0.18R$ was arbitrary defined. The variations in the axial linear velocities in a column cross-section are given as the ratio between the mean linear velocity in the wall region and the linear velocity at the centre of the column ($\bar{U}_{wall}/U_{centre}$).

4.3.1. The influence of the flow rate

Typical computed variations of the interstitial void fraction are shown in Fig. 10 and corresponding velocity variations are shown in Figs. 11 and 12. The void fraction decreases along the column and the linear velocity increases due to the successive compaction of the bed caused by the fluid stress according to Figs. 10 and 11. The relatively lower degree of compaction at the wall, close to the outlet of the column, can be understood by recalling that the wall friction opposes the compaction and this effect is largest at the wall. At the inlet, on the other hand, a higher degree of compaction is predicted close to the wall than at the centre (Fig. 10). This is a consequence of the fact that the chromatographic bed is assumed to be under piston stress and that the bed height is assumed to be uniform. The corresponding radial variations in linear velocity (U/U_{centre}) are shown in Fig. 12. The variations in linear velocity and void fraction showed a similar pattern in all presented simulations.

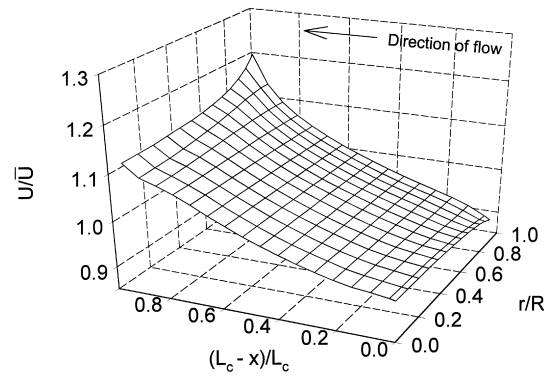

Fig. 11. Computed, normalized, interstitial axial velocity. U = local linear velocity and $\bar{U}$ = average linear velocity. Parameters: $q = 0.26$ ml/s, $R = 0.0565$ m, $L_c = 0.313$ m, $\varepsilon_{mean} = 0.237$, $\mu = 0.001$ Pa s, $\rho = 1000$ kg/m^3. The pressure drop was 2.18 kPa.

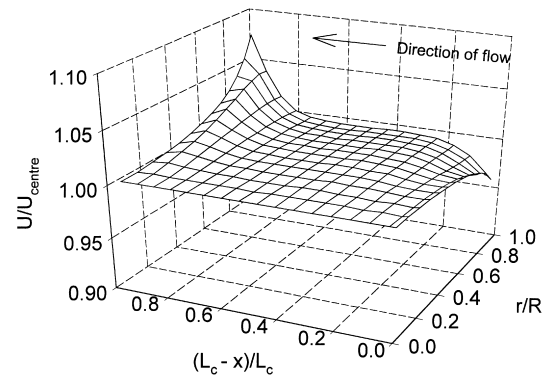

Fig. 12. Computed, normalized, interstitial axial velocity. Radial variations. Parameters: $q = 0.26$ ml/s, $R = 0.0565$ m, $L_c = 0.313$ m, $\varepsilon_{mean} = 0.237$, $\mu = 0.001$ Pa s, $\rho = 1000$ kg/m^3. The pressure drop was 2.18 kPa.

Fig. 13 shows the variation of the linear velocity ($\bar{U}_{wall}/U_{centre}$) at different flow rates. The predicted ratio of the linear velocity in the wall region to that at the centre varied between 0.95 and 1.4 and was typically around 0.97

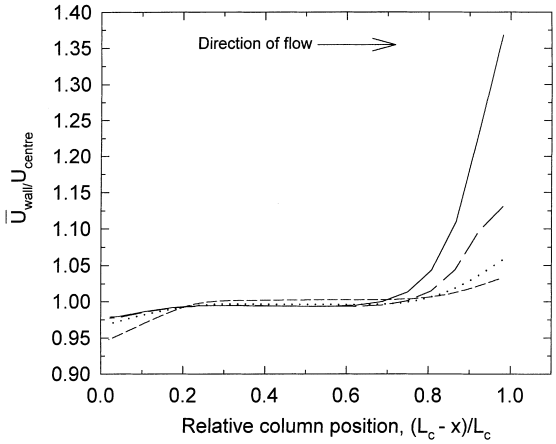

Fig. 13. Computed variation in the linear velocity (U) in the wall region ($\Delta r = 0.18R$) compared with that at the centre for different flow-rates. (- - -) $U_{mean} \approx 0.5 \times 10^{-8}$ m/s, (· · ·) $U_{mean} = 1.15 \times 10^{-4}$ m/s, (– – –) $U_{mean} = 1.76 \times 10^{-4}$ m/s, (———) $U_{mean} = 1.87 \times 10^{-4}$ m/s. The mechanical properties are those given in Table 2. Parameters in common were: $R = 0.0565$ m, $L_c = 0.313$ m, $\mu_f = 0.16$, $\mu = 0.001$ Pa s, $\varepsilon_{mean} = 0.237$, and $\rho = 1000$ kg/m^3.

close to the inlet of the column and between 1.03 and 1.4 close to the outlet. At low flow rates the velocity variations are largest at the inlet due to the relatively big influence of the mechanical stress. At high flow rates large velocity variations are found close to the outlet of the column due to the relatively big influence of the fluid stress. The predicted shift in the velocity profile with increasing flow rate is, as previously discussed, due to the influence of the end pieces of the column in combination with the presence of a frictional force at the wall. The non-linear dependence of the permeability on the interstitial void fraction (Eq. (7)) also contributes to the velocity profile through a column cross-section and its variation with location in the column and degree of compaction.

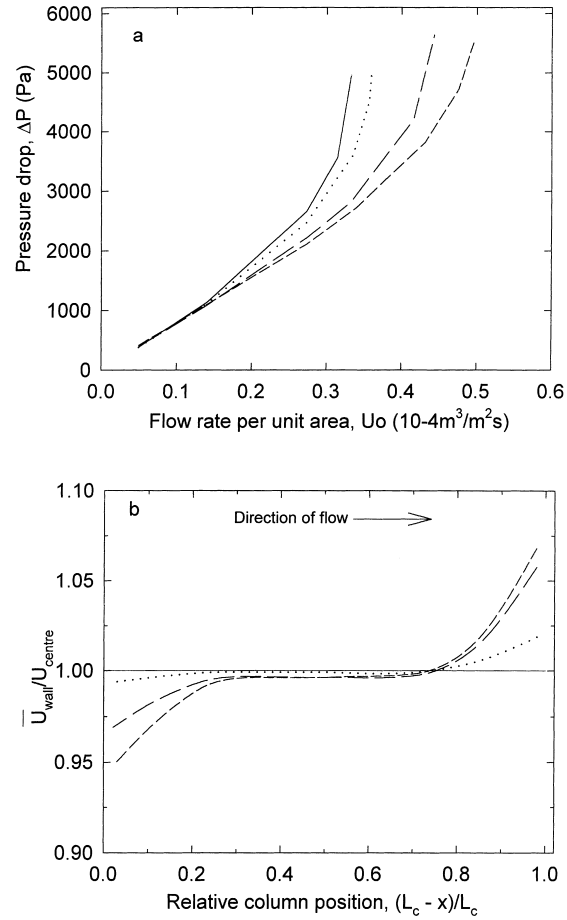

Fig. 14. Computed pressure drop vs. superficial velocity (U_0) for different wall friction coefficients and (b) computed variation in the linear velocity (U) in the wall region ($\Delta r = 0.18R$) compared with that at the centre of the column for different wall friction coefficients for $\bar{U} = U_{column} = 1.15 \times 10^{-4}$ m/s; (- - -) $\mu_f = 0.24$, (– – –) $\mu_f = 0.16$, (· · ·) $\mu_f = 0.04$, (———) $\mu_f = 0$. Parameters in common were: $R = 0.0565$ m, $L_c = 0.313$ m, $\varepsilon_{mean} = 0.237$, $\mu = 0.001$ Pa s and $\rho = 1000$ kg/m^3.

4.3.2. The influence of the wall friction coefficient

The wall friction decreases the solid stress to which the matrix is exposed and consequently, at a given flow rate (U_0), high wall friction will cause the column to be compressed less than a column characterized by low wall friction. The computed maximum possible flow rate will increase with increasing wall friction according to Fig. 14(a). For example, in a column ($R = 0.0565$) with a wall friction coefficient of 0.16 a 30% higher flow rate is possible, compared with a column with zero wall friction (Fig. 14(a)). The cost of the increase in flow rate is, however, an increase in the variation of the linear velocity (U) through a cross-section of the column. Large wall friction coefficients will generally cause larger variations than small wall friction coefficients (Fig. 14(b)).

4.3.3. The influence of the column radius

The influence of the wall friction is highly dependent on the column radius. Simulated flow–pressure curves for different column radii ($\mu_f = 0.16$) are presented in Fig. 15(a). In a narrow column, the chromatographic bed was found to be greatly stabilized and high flow rates (U_0) could be obtained, while in wider columns the influence of the wall friction coefficient was small and low flow rates were obtained. At a column radius being 0.3 m ($L_c/D = 0.5$) the pressure drop at a given flow rate will change very little according to the simulation as the column radius is further increased. This is in qualitative agreement with experiments performed on agarose-based chromatographic packings ($L_c = 0.15$ m), where only small differences in performance were found as the L_c/D ratio decreased from 0.4 to 0.25 [1]. At higher L_c/D ratios large differences were found [1].

The variations in the linear velocity in a column cross-section at different axial positions are shown in Fig. 15(b). In a narrow column, the stress gradients are expected to be small since the wall friction is felt through the whole cross-section of the column. This is also the case in our simulation, with the exception of a small region close to the inlet, where

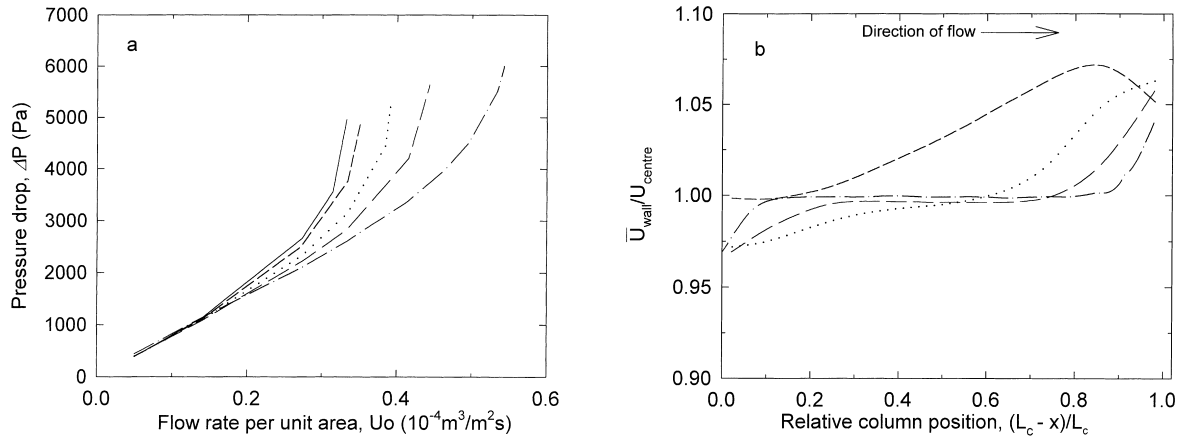

Fig. 15. Computed pressure drop vs. superficial velocity (U_0) for different column radii and (b) computed variation in the linear velocity (U) in the wall region ($\Delta r = 0.18R$) compared with that at the centre of the column for different column radii for $\bar{U}_{\text{column}} = 1.15 \times 10^{-4}$ m/s; (–·–·–) $R = 0.03$ m, (– – –) $R = 0.0565$ m, (· · ·) $R = 0.1$ m, (- - -) $R = 0.3$ m. (———) $R \to \infty$. Parameters in common were: $L_c = 0.313$ m, $\varepsilon_{\text{mean}} = 0.237$, $\mu_f = 0.16$, $\mu = 0.001$ Pa s and $\rho = 1000$ kg/m^3.

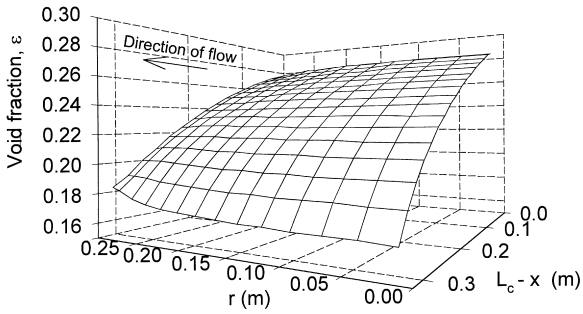

Fig. 16. Variations in void fraction in a wide column ($D/L_c = 0.5$). $R = 0.30$ m, $L_c = 0.313$ m, $\mu_f = 0.16$, $\varepsilon_{\text{mean}} = 0.237$, $\mu = 0.001$ Pa s and $\rho = 1000$ kg/m^3.

a fairly high variation in the linear velocity was found, compared with the rest of the column. At larger column radii, the wall friction is felt to a lesser extent at the centre of the column, leading to larger radial void/stress variations and consequently larger velocity variations than in narrow columns. It is interesting to note that at a column radius being 0.3 m large velocity variations are predicted even though the pressure drop is predicted to be essentially independent of the column radius. Eventually, as the column radius is increased further, the influence of the wall friction will decrease. In the widest column ($R = 0.3$ m) the variation in the linear velocity decreases at the outlet of the column. This flow pattern is due to rapidly developing axial as well as radial void gradients according to Fig. 16.

5. Conclusions

The flow through and the compression of a chromatographic gel packed in a column has been characterized experimentally and theoretically using a two-dimensional model based on the assumption of pure elastic deformation according to Biot [13].

Pressure profiles along the column at different flow rates were well predicted by the model. At low and moderate flow rates, flow–pressure curves for columns of different lengths and different void fractions were predicted successfully. These results indicate that the model adequately describes the most important features of compaction and flow through a non-rigid chromatographic column.

By performing computer simulations, pressure drop and linear velocity variations were investigated by assuming different wall friction coefficients and column radii. The largest velocity variations in a column cross-section were found, as expected, close to the column wall, near the outlet and inlet of the column. The simulations showed that velocity variations in a column cross-section in the range of 10% are likely to occur, which, according to Yun and Guiochon [2], may influence the chromatographic band profiles. The simulations presented also point to a necessity for two-dimensional experimental investigations in order to verify and further develop the model.

Finally, we have demonstrated the usefulness of a two-dimensional model in understanding the complex stress and flow situation in a compressible chromatographic bed under piston stress. From a practical point of view, we also believe that these types of calculations may be useful in a scale-up situation, as the limits of different chromatographic media and chromatographic equipment can be investigated.

6. Nomenclature

d_p	particle diameter (m)
E	Young's modulus (Pa)
G	shear modulus (Pa)

g	gravitational acceleration (m/s^2)
L_c	column length (m)
L_{co}	column length before compression (m)
k	permeability coefficient (m^2)
p	fluid pressure (Pa)
P	pressure (see Eq. (1)) (Pa)
q	flow rate (ml/s)
R	column radius (m)
r	radial position (m)
t	time (s)
U	linear velocity (m/s)
$\bar{U}$	mean linear velocity (m/s)
U_0	flow per unit area, superficial velocity (m/s)
u	displacement of solid phase (m)
x	axial position (m)

Greek letters

ε'	strain in solid phase (–)
ε	intergranular void fraction (–)
μ	viscosity (Pa s)
μ_f	wall friction coefficient (–)
ν	Poisson's ratio (–)
ρ	density (kg/m^3)
σ	stress in solids phase (Pa)
σ_w	shear stress at the wall (solid phase) (Pa)

Subscripts

x, y, z	directions in a Cartesian coordinate system
r	radial direction

Acknowledgements

The authors wish to acknowledge the financial support made available for this study by the Swedish Board for Technical and Industrial Development and are indebted to Amersham Pharmacia Biotech AB, Sweden for supplying the chromatographic media and the columns.

References

[1] G.K. Sofer, L.E. Nyström, Process Chromatography, A Practical Guide, Academic Press, London, UK 1989.
[2] T. Yun, G. Guiochon, J. Chromatogr. A. 672 (1994) 1–10.
[3] M.K. Jostrua, A. Emnéus, P. Tibbling, in: H. Peeters (Ed.), Protides of the Biological Fluids, vol. 15, Elsevier, Amsterdam, 1967, pp. 575–579.
[4] P.A. Davies, B.J. Bellhouse, Chem. Eng. Sci. 44 (1989) 452–455.
[5] F.H. Verhoff, J.J. Furjanic, Ind. Eng. Chem. Process. Des. Dev. 22 (1983) 192–198.
[6] K.C.E. Östergren, C. Trägårdh, G.G. Enstad, J. Mosby, AIChE. J. 44 (1998) 2–12.
[7] K. Östergren, C. Trägårdh, Numer. Heat Transfer, Part A. 32 (1997) 247–265.
[8] J-C. Jansson, P. Hedman, in: A. Fiechter (Ed.), Advances in Biochemical Engineering, Springer, Berlin, 1982, pp. 43–99.
[9] W.L. McCabe, J.C. Smith, Unit Operations of Chemical Engineering, McGraw-Hill, Tokyo, 1983, pp. 809–817.
[10] F.M. Tiller, W-M. Lu, AIChE. J. 18 (1972) 569–572.
[11] M. Shirato, T. Aragaki, R. Mori, R.K. Sawamoto, J. Chem. Eng. Jpn. 1 (1968) 86–90.
[12] A.W. Jenike, Bulletin No. 123, Utah Engineering Experiment Station, University of Utah, 1964.
[13] M.A. Biot, J. Appl. Phys. 12 (1941) 155–164.
[14] R.W. Lewis, B.A. Schrefler, The Finite Element Method in the Deformation and Consolidation of Porous Media, Wiley, UK, 1987.
[15] A. Verruijt, in: A.J.M. DeWiest (Ed.), Flow Through Porous Media, Academic Press, New York, 1969, pp. 331–376.
[16] J. Bear, Dynamics of Fluids in Porous Media, American Elsevier, New York, 1972.
[17] K. Östergren, C. Trägårdh, in: D.L. Pyle (Ed.), Separations for Biotechnology 2, Elsevier Applied Science, UK, 1990, pp. 632–641.
[18] Pharmacia LKB Biotechnoligy, Gel filtration Theory and practice, Lund, Sweden, 1990.
[19] K. Ueyama, S. Furasaki, Chem. Eng. Commun. 36 (1985) 299–316.
[20] P. Flodin, Dextran gels and their applications in gel filtration, Meijels Bokindustri, Halmstad, Sweden, 1963.
[21] J. Mosby, G.G. Enstad, POSTEC Report No. 931113-3, Porsgrunn, Norway, 1993.